



Electron pair emission from a Pb surface at room temperature

Y. Aliaev, I. Kostanovskiy*, J. Kirschner, F.O. Schumann

Max-Planck-Institut für Mikrostrukturphysik, Weinberg 2, Halle 06120, Germany



ARTICLE INFO

Keywords:

Auger electron spectroscopy
Electron emission
Photoelectron emission
Auger photoelectron coincidence spectroscopy

ABSTRACT

We provide a comprehensive study of the electron pair emission from a Pb surface at room temperature. We excited the sample via a primary electron beam or laboratory light source. Besides the excitation of the 6s and 6p valence states the weakly bound 5d core levels are accessible. This allows us to investigate the Auger-photoelectron pairs in coincidence. The electron pair excitation spectra can be largely explained by the underlying electronic structure. Varying the primary energy changes the relative contribution of the 6s and 6p states. The measured double photoemission intensity is dominated by the emission of 5d photoelectrons and the resulting Auger electron. The Auger electron line shape has mainly contributions due the 6p electrons, because the 6s electrons can not lead to the emission of an Auger electron due to energy conservation. From the sum energy spectra we find that the effective Coulomb interaction U_{eff} is close to zero. The double photoemission intensity without participation of the 5d levels displays rather featureless spectra. Among the materials which display superconductivity is Pb. The explanation of this effect requires the introduction of Cooper pairs. It was theoretically predicted that double photoemission of Cooper pairs is possible. We discuss the experimental feasibility of such measurements.

1. Introduction

The properties of matter are decisively determined by the electronic structure. Electrons do not move independently within a solid, but exert a mutual influence via the Coulomb interaction and the Pauli principle. A complete microscopic description of all electrons is impossible. However, it turns out that it is possible to cast the effects of the electron-electron interaction into a mean-field type description. This is also known as the quasi-particle picture. Hence, the access to the underlying electronic structure via photoelectron spectroscopy has been proven very successful. Nevertheless it is desirable to investigate the mutual relations between electrons. This is possible via electron pair emission from surfaces, because the existence of this effect requires a finite electron-electron interaction. It is customary to distinguish between primary electron and photon absorption as (e,2e) and Double photoemission (DPE), respectively.

We have decided to investigate a Pb surface because of particular features in the electronic states. The valence band of Pb has contributions from the 6s and 6p levels which are separated by a gap of 3.1 eV. This means in contrast to transition metals there is no hybridisation between electrons from different orbitals. The spin-orbit split 5d levels possess a binding energy of around 20 eV. This means (e,2e) experiments with typical excitation energies in the range of 30–60 eV can

excite these core levels leading to autoionization states. This aspect is not included in the current theory of (e,2e) and in experiments on other materials core levels were more tightly bound and not excited.

The shallow 5d core levels can also be excited by a laboratory UV light source leading to the emission of 5d photoelectrons and Auger electrons. Although some results have been published using X-ray laboratory sources most studies are conducted using synchrotron radiation [1–5]. We explore the DPE process with and without participation of the 5d core level.

The (e,2e) energy spectra show features which can be largely understood on the basis of the bulk density of states (DOS). The relative contributions of the 6s and 6p valence states and the energy sharing does depend on the primary energy E_p . We find evidence that the 5d levels play a role via an autoionization pathway. We observe that the DPE intensity is dominated by the emission of Auger-photoelectron pairs. From the Auger lineshape we determine that the effective Coulomb correlation U_{eff} is close to zero. The DPE intensity directly from the valence band is an order of magnitude smaller than those of the Auger-photoelectron pairs. This would be consistent with a small value of the Coulomb correlation within the valence band [6,7].

Our experiments were performed at room temperature where Pb is not superconducting. The explanation of superconductivity requires the concept of Cooper pairs. The possibility of Cooper pair emission via

* Corresponding author.

E-mail address: ilya.kostanovskiy@mpi-halle.mpg.de (I. Kostanovskiy).

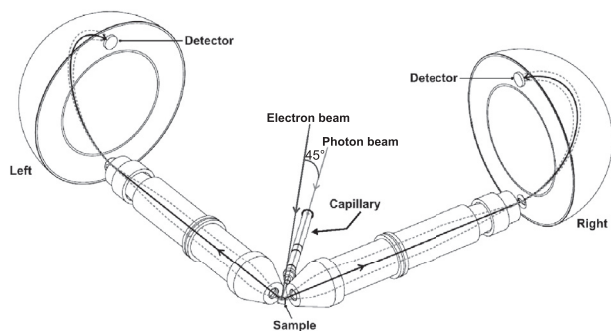


Fig. 1. The two transfer lenses of the spectrometer are symmetrically aligned with respect to the surface normal. The photon beam propagates along the surface normal. An electron gun for (e,2e) experiments was available, this primary beam has an angle of 45° with respect to the scattering plane.

single photon absorption has been theoretically predicted [8–10]. We use our data to assess whether this effect can be experimentally observed if the sample is in the superconducting state. We are motivated to address this issue, because of the potential new insights on the pairing mechanism. We find the expected emission rates to be prohibitive. We conclude that only more recent electron spectrometer using the high acceleration voltage of cathode lenses promise success.

2. Experimental details

The details of the coincidence spectrometer have been described in more detail elsewhere [11–13]. Therefore we recall only the main aspects. The general layout in Fig. 1 shows two hemispherical electron energy analyzers with a mean radius of 200 mm. They are equipped with wide angle transfer lenses and position sensitive detectors. We label the spectrometers as ‘left’ and ‘right’ respectively. We will quote the kinetic energy with respect to the vacuum level of the sample. The two electron-optical axes of the transfer lenses include an angle of 90° and define the reaction plane, in which the primary photon beam lies. The emitted electrons are detected with energies E_{left} and E_{right} . Due to the entrance slits not all electrons which enter the lens will be detected. The orientation of the slits of each spectrometer has a $\pm 15^\circ$ acceptance within the scattering plane.

All experiments were performed with the photon beam being parallel to the normal which has an angle of 45° with respect to the optical axis of the two transfer lenses. The sample position was maintained during the (e,2e) experiments for which an electron gun was available. The primary electron beam had an angle of 45° with respect to the scattering plane, see Fig. 1. For in-house experiments the system has been upgraded by the attachment of VUV light source which consists of a He lamp and a toroidal monochromator [6,14,15]. We used the He II lines at 40.8, 48.4 and 51.0 eV, respectively. Space constraints do not allow to have the sample at the focus point of the grating. Therefore, we fitted the exit arm of the monochromator with an additional capillary of 200 mm length and 2 mm diameter. This has the added benefit of improved differential pumping. The partial pressure of He during normal operation is $2-3 \times 10^{-10}$ mbar, while the base pressure was 5×10^{-11} mbar. In order to reduce the primary flux on the sample we placed a set of apertures between the He light source and the monochromator.

We are interested in those events in which a single photon (electron) leads to the emission of an electron pair which we term ‘true’ coincidences. However, it is also possible that two photons (electrons) lead to the individual emission of single electrons which will be recorded by the coincidence electronics. These unwanted events are usually termed ‘random’ coincidences. The ‘true’ coincidences scale linearly with the primary flux, while the random ‘random’ contribution scales quadratically. This allows us to reduce the latter to an acceptable level. This

comes at the expense of a low coincidence count rate. Following standard procedures documented in the literature we are able to remove the aggregate effect of the ‘random’ coincidences [4,16]. The implementation of these procedures for our coincidence spectrometer has been explained previously [13]. At this point we can state that we are able to determine the ‘true’ coincidence rate and energy spectra.

We operated the spectrometer with a pass energy of 150 eV which results in an energy window of 13 eV which can be covered with each spectrometer. The slit size selected was 1 mm, this leads to an energy resolution of 0.35 eV of each spectrometer. The line width of the VUV light (a few meV) can be neglected while the primary electron energy has a width of 0.3 eV. We keep all voltages of the electron-optical components constant for a given coincidence experiment. The sample was a polycrystalline Pb foil which was cleaned via Ar⁺ sputtering and annealing up to 150 C°. Auger spectroscopy verified the cleanliness of the surface. The lowest temperature of the manipulator is 120 K. We chose to perform all measurements at room temperature, because the temperature broadening is still smaller than the selected spectrometer resolution. For absolute energy calibration we use the recent work of Iablonsky et. al on polycrystalline and atomic Pb [17].

3. Results and discussion

3.1. (e,2e) experiments

In our experiments two electrons are emitted from a surface which possess kinetic energies E_{left} and E_{right} , respectively. In the following we quote these energies with respect to the vacuum level of the sample. This pair can also be characterized by the energy sum $E_{sum} = E_{left} + E_{right}$. In an (e,2e) experiment a valence electron with binding energy E_B is emitted after a primary electron with kinetic energy E_p impinges onto the surface. Effectively this process removes one electron from the sample, hence the work function of the surface ϕ has to be considered. Therefore, energy conservation for an (e,2e) process can be formulated as:

$$E_p + E_B = E_{sum} + \phi \quad (1)$$

In the DPE process, a photon with energy $h\nu$ is absorbed by the sample and two electrons with binding energies E_{B1} and E_{B2} are emitted. Therefore, in the energy balance the work function has to be entered twice and we obtain:

$$h\nu + E_{B1} + E_{B2} = E_{left} + E_{right} + 2\phi = E_{sum} + 2\phi \quad (2)$$

A useful reference energy is the maximum sum energy E_{sum}^{max} which is obtained if the emitted electrons originate from the Fermi level E_F . From the previous definition it follows that in a (e,2e) process $E_{sum}^{max} = E_p - \phi$. For a DPE process it readily follows $E_{sum}^{max} = h\nu - 2\phi$. In the last step we have assumed that the energy required to remove an electron pair is equal to twice the energy to remove a single electron. This can only be an approximation, because the electron correlation is ignored at this point. A prominent example may illustrate this. The energy required for single ionization of the He atom is 24.59 eV. For double ionization an energy of 79.01 eV is needed, which is very different from twice the single ionization energy. Similarly, for Auger electron emission it is known that the kinetic energy can be significantly shifted from the position expected by using the binding energies of the involved states. This shift can be identified with an effective electron-electron interaction strength U_{eff} [18]. In the case of Cu a value of 8 eV is reported. This is the additional energy besides twice the work function which needs to be furnished in order to remove two 3d valence electrons.

The operator leading to single photoelectron emission is the dipole operator, the equivalent for double photoemission is the sum of two dipole operators [19,20]. The evaluation of the transition matrix element with single particle wave functions leads to a vanishing DPE intensity [19,20]. The presence of the electron-electron interaction

mandates a formulation of a correlated two-particle wave function. This means the wave function must explicitly depend on the coordinate difference of two electrons. Therefore, DPE is particularly sensitive to the electron-electron correlation. In a recent theoretical work using a Hubbard Hamiltonian it was shown that the DPE intensity scales quadratically with the Hubbard parameter U [7]. An experimental study on a variety of materials including ferromagnets and transition metal oxides indicated intensity relations [6]. Transition metal oxides like NiO and CoO revealed a significantly higher count rate than metals like Cu and Ag.

In the pair emission process from crystalline surfaces also the conservation of the in-plane momentum (modulo a reciprocal lattice vector) has to be fulfilled. The emission direction and kinetic energy of the outgoing electrons constrain which valence states are involved in the emission.

At this point it is useful to recall the basics of the (e,2e) theory from surfaces [22–26]. The initial state is given by the incoming primary electron while the valence electron is described by a Bloch state. The two outgoing electrons are time-reversed LEED states. A consequence of energy and momentum conservation is that the emission direction and kinetic energy of these outgoing electrons define the momentum and binding energy of the valence state involved in the (e,2e) process. The actual (e,2e) process is described by a screened Coulomb interaction among the outgoing electrons. Although there is no substitute for a proper (e,2e) calculation, we have shown experimentally that for crystalline metallic surfaces the kinematical accessible band structure alone provides a fair description of the spectra [13,27,28]. In this simplification we assume a constant matrix element for the transition. This captures essential parts of the sum energy spectrum, namely the position of the intensity maxima. The relative intensity between maxima can only be understood with a proper (e,2e) calculation. The information about the in-plane momentum is lost if a polycrystalline sample is used. Hence the experiment will effectively integrate over the whole Brillouin zone. Hence rather than discussing the electronic bandstructure $E(k)$ the density-of-states (DOS) is of relevance.

In Fig. 2 we present the theoretical occupied electronic density-of-states DOS for bulk lead from Würde et al. [21]. The axis is the binding energy with the Fermi level E_F at $E_B = 0$. Additionally we have included the DOS convoluted with 0.7 eV wide Gaussian to take into account the energy resolution of the coincidence experiment. It is apparent that the 6s and 6p levels are separated by a 3.1 eV wide gap. Therefore hybridisation between these levels can be ignored. The 6s band is located in a region of 6.8–11.4 eV below E_F , while the occupied 6p band extends from $E_B = 3.9$ eV to E_F . The unoccupied region of the 6p band reaches up to 7 eV above E_F .

In Fig. 3 we present a series of 2D-Energy spectra of (e,2e) experiments excited with different primary energies. In all plots we have included a diagonal black line which marks the position of E_{sum}^{max} . The pair of dashed diagonal lines indicates the energetic position of the band gap separating the 6s and 6p levels. Therefore, we expect no intensity in this region. However, it is apparent that the experiment detects a significant contribution. For $E_p = 32.8$ eV the intensity near E_{sum}^{max} is highest if one electron is fast while the other is slow. This is in contrast to the other data shown in Fig. 3(b) and (c) where the intensity is more uniform along the E_{sum}^{max} line.

For a more detailed discussion it is useful to present the E_{sum} spectra obtained by different primary energies E_p , see Fig. 4. For a better comparison we plot the intensity as a function of the two-particle binding energy $E_B^{2e} = E_{sum}^{max} - E_{sum}$. This choice ensures that the same valence states show up at the same energy position as it is customary in photoemission. In all spectra we also included the convoluted DOS shown in Fig. 2. We adjusted the intensity levels of the DOS such that the peak at $E_B = 2.5$ eV matches the intensity of the experiment. The DOS peak near E_F shows up only as a shoulder, clearly a proper discussion requires a realistic (e,2e) calculation.

Although the DOS displays more fine-structure in the 6p region, the

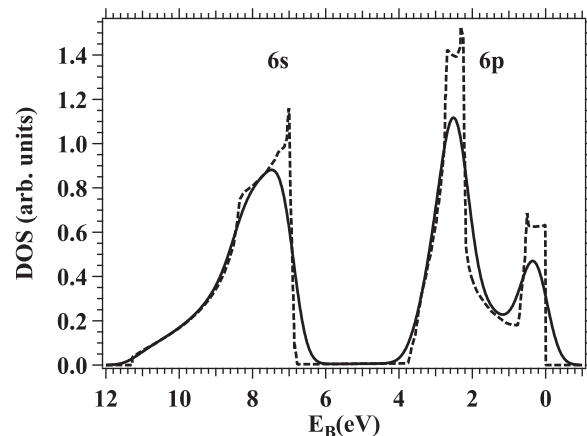


Fig. 2. The dashed line depicts the bulk DOS as given by Würde et al. [21]. The solid line is the convolution of the DOS with a Gaussian. It has a width of 0.7 eV which is the energy resolution of the (e,2e) coincidence experiment.

E_{sum} spectra in this range are reasonably reproduced. We also note the shape of 6p region is hardly affected by the value of E_p . The variation of E_p mainly changes the contribution of the 6p region to the overall intensity. In previous (e,2e) works on Cu(111) and Cu(100) surfaces we observed that the contributions from the 3d and 4sp states depend strongly on the value of E_p [13,28]. This we explained via diffraction of pairs, which could also be of relevance in the current work.

According to the DOS there are no available valence states in the gap between interval 3.9 to 6.8 eV, see Fig. 2. Yet there is significant (e,2e) intensity. As far as valence band photoemission via UPS and XPS is concerned there is also intensity in this region [29–32]. In these studies the intensity within the gap region amounts to roughly a quarter of the 6p region. We will provide an explanation for the coincidence intensity within the gap region. It is based on the excitation of the 5d core levels and the subsequent electron emission. In a first step we want to demonstrate that the emission of a 5d core electron and scattered primary can be identified. In preparation of the discussion we show a level diagram in Fig. 5 which uses the DOS shown in Fig. 2. We have added the DOS of the 5d states schematically but not to scale. A primary electron can excite a 5d core electron, therefore it will suffer an energy loss. The smallest loss is given if the least bound $5d_{5/2}$ level with binding energy $E_B^{5/2}$ is excited to the Fermi level. This is indicated by the left dashed arrow in Fig. 5. Consequently we can write for the energy of the scattered primary:

$$E_{sc}^a = E_p - E_B^{5/2} \quad (3)$$

The scattered primary will possess less energy if the core electron is excited above the vacuum level. As an example we consider the $5d_{3/2}$ as sketched by the right dashed arrow in Fig. 5. Let us suppose the core electron has a kinetic energy of E_k while the work function is ϕ . In this case the energy of the scattered electron energy can be written as:

$$E_{sc}^b = E_p - E_B^{3/2} - \phi - E_k \quad (4)$$

The sample is now in an autoionizing state and an electron from the valence band will fill the vacancy and Auger emission sets in. We will show below that this Auger electron emission exists.

As an example we plot (e,2e) data in Fig. 6(a), the 2D-Energy spectrum was obtained with $E_p = 69.8$ eV. The contribution from the valence states is essentially out of the spectrometer window and with it the position of the E_{sum}^{max} line. We can clearly observe a pair of diagonal intensity features, which reside on a substantial background. In Fig. 6 (b) we present a E_{sum} spectrum derived from the data shown in Fig. 6 (a). We can see two peaks at the two-particle binding energies of 20.58 and 17.93 eV, respectively. These values agree with the known binding energy values of the 5d core levels [17]. Therefore, we have detected

the scattered primary electron and the excited $5d$ electron.

We have performed also experiments at higher E_p values up to 116 eV. The E_{sum} spectra all display the double peak due to the spin-orbit split $5d$ levels. Increasing the primary energy will decrease the background to some extent. For E_p values below 69.8 eV the diagonal feature can not be observed anymore. This should not be taken as a threshold value for this process to occur.

Suppose the $5d_{3/2}$ electron is to leave the surface with $E_k=0$ eV due to a primary electron collision. The minimum primary energy is given by Eq. (4). The numerical value is $E_p = 24.58$ eV. In this case two electrons with zero kinetic energy are emitted. For larger E_p values the excess energy can be shared among the emitted core electron and scattered primary. For example if the primary energy is increased by 32 eV to $E_p = 56.58$ eV the energy sum of the scattered primary and $5d_{3/2}$ electron is 32 eV. From this point of view we should expect the emergence of a diagonal intensity region similar to Fig. 6. In order to capture the largest part of this signature both spectrometer should be set to a central energy of 16 eV. However, doing so will also allow the detection of an Auger electron after filling the $5d$ vacancy, we will demonstrate below that the Auger electron covers an energy window from 6.3–16.3 eV, see Fig. 8. This means the excitation of a core-electron via a primary electron scattering can lead to the emission of three electrons. Namely, the excited core electron, the inelastically scattered primary electron and the Auger electron. Our spectrometer detects only two electrons in coincidence. Hence, if one of the detected electrons is the Auger electron this pair will not contribute to the intensity within the diagonal region. The diagonal intensity feature only shows up if the scattered primary and $5d$ core electron are detected. The emergence of the Auger electron within the spectrometer window should result in an almost constant intensity for $E_p=56.7$ eV. This is indeed our observation. The data shown in Fig. 6 were obtained with $E_p=69.8$ eV and the central energy of the spectrometer is 22 eV. This has the consequence that the Auger electrons can only be detected in the lower left hand corner. Hence their effect on the diagonal intensity band can be ignored. We return now to the question why the (e,2e) data presented in Fig. 3 show significant intensity with in the gap region. We suggest a two-step scenario in which the scattered primary is detected in coincidence with the Auger electron. Furthermore, we want to consider only those excited core electron which posses a kinetic energy below the low energy cut-off for a given spectrometer setting. For the data obtained with $E_p=32.8$ eV this cut-off is 6.3 eV, see Fig. 3 (a). This means that excitation of a $5d_{3/2}$ electron just below this energy leads to a scattered primary electron energy of 1.8 eV. This follows immediately from Eq. (4). The excitation of the $5d_{5/2}$ to the Fermi level leads to the scattered primary energy of 14.8 eV, see Eq. (3). This means the scattered electron can posses an energy in the interval from 1.8 to 14.8 eV. However, since the lowest detectable energy is 6.3 eV we need to consider only the interval 6.3 eV to 14.8 eV. As we will show below the Auger electron due to filling the $5d$ vacancy covers a kinetic energy window from 6.3 to 16.3 eV.

Now we go through all combinations of the kinetic energy of the Auger and scattered primary. Furthermore, we ensure that the sum energy of these combinations do not exceed E_{sum}^{max} . For simplicity we assume that each combination occurs with the same probability. One can visualize the result within a 2D-Energy plot, see Fig. 7. The red area is the region which is covered by the different combinations. The solid diagonal line is the E_{sum}^{max} while the pair of dashed diagonal lines mark the gap region of the DOS. This is analogous to Fig. 3 (a). It is apparent that the area bounded by the pair of dashed lines is almost covered by the red region. This means that the two-step process can largely explain the intensity in this region. Equivalent results are obtained for $E_p=40.4$ and 44.4 eV.

While the current (e,2e) theoretical framework for surfaces works rather well, the contribution of core levels is not included. For almost all of the theoretical and experimental (e,2e) studies this was not a severe problem, because the primary energy was not sufficient to excite

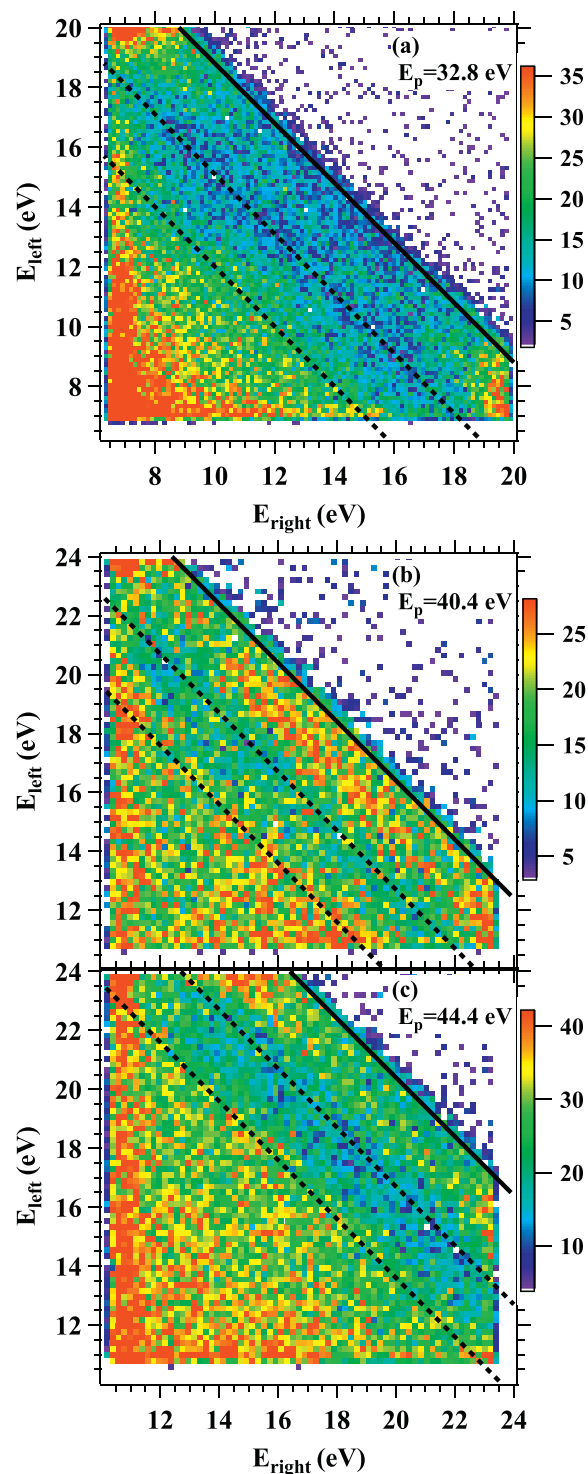


Fig. 3. 2D-Energy distribution for (e,2e) obtained with $E_p=32.8$, 40.4 and 44.4 eV, respectively. The solid diagonal line indicates the position of E_{sum}^{max} . The pair of dashed lines show the position of the energy gap.

a core level [13,23–26,28,33–36]. This is not the case of Pb and an autoionizing pathway needs to be considered in the light of the strong intensity contribution which occurs in the energy region of the gap.

3.2. Auger-photoelectron pairs

We begin our discussion of the pair emission due to photon absorption with Fig. 8. There we display the 2D-Energy distributions of

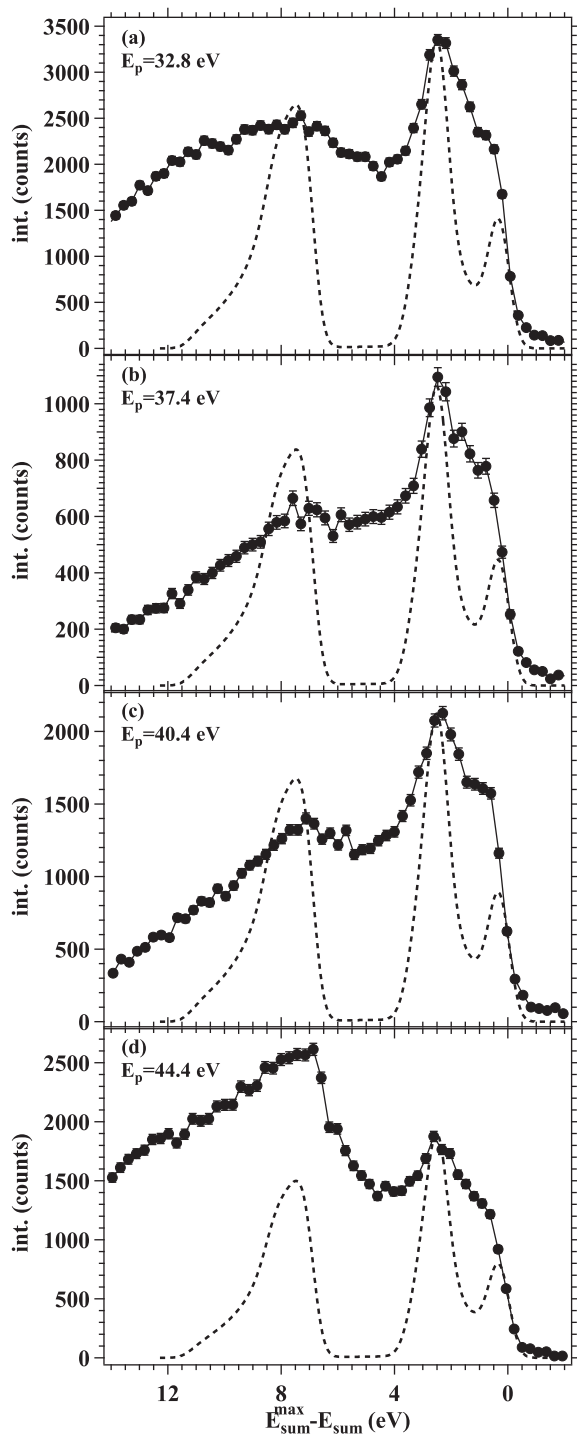


Fig. 4. Sum energy spectra for (e,2e) experiments for a variety of primary energies. The dashed line is the bulk DOS of Pb convoluted with 0.7 eV wide Gaussian, see Fig. 2.

the DPE experiment with a photon energy of 40.8 and 48.4 eV, respectively. In panel (a) we can see prominent intensity regions which are aligned parallel to the x- and y-axis. These stem from excitations of the spin-orbit split 5d electrons and subsequent Auger decay. The kinetic energy of the $5d_{3/2}$ photoelectron is 16.3 eV while the $5d_{5/2}$ line can be found at 19.0 eV. The line width is mainly limited by our energy resolution of about 0.35 eV. The center of the Auger lines are at around 10–11 eV and their width is about 8 eV. This larger width simply reflects the fact that in this Auger decay two valence electrons participate.

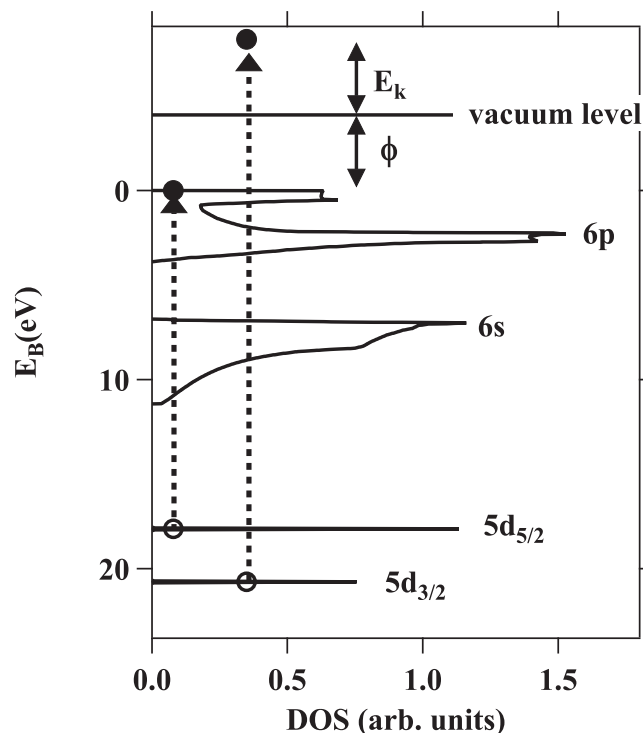


Fig. 5. In this schematic energy diagram of Pb we show with the left dashed arrow that a primary electron can excite a $5d_{5/2}$ electron to the Fermi level. The energy loss of the primary electron is simply the $5d_{5/2}$ binding energy. It is also possible that the core electron is excited above the vacuum level by an amount E_k , as indicated by the right dashed arrow. In this case the primary electron has to furnish the binding energy, work function ϕ and energy E_k . Upon excitation of the core electron the sample is in an autoionizing state and will decay via the emission of an Auger electron, see Fig. 8.

We come back to this point later.

We notice also a broad intensity maximum centered roughly at 10 eV/10 eV. At first sight it appears that this is due to the emission of two Auger electrons. This is of course not possible with a single photon. The origin of this feature is a coincidence between an Auger and photoelectron where the latter has suffered energy losses and has the same kinetic energy as the Auger electron. These two electrons with the same kinetic energy can be recorded in two different ways. First, the Auger electron is detected by the left spectrometer and the scattered photo electron by the right one. Second, the role of the two spectrometers is exchanged. This leads to an apparent double counting in the 2D-Energy distribution which disappears in a E_{sum} spectrum [37].

In order to capture the Auger-photoelectron pairs with $h\nu = 48.4$ eV it is necessary to change the settings of one spectrometer. Now the left spectrometer measures the 5d photoelectrons while the right spectrometer detects the Auger electron, see Fig. 8 (b). Therefore we see only the horizontal intensity bands in contrast to Fig. 8 (a).

The Auger transition we observe involves two valence electrons. This so-called CVV Auger process was subject of a variety of experimental studies using single electron photoemission [38–42] or coincidence spectroscopy [1–3,43,44]. A solid theoretical framework was formulated by Cini and Sawatzky [39,45]. Within this theory the influence of the electron-electron interaction U in the valence band onto the Auger line shape can be calculated. The relevant expression leads for $U = 0$ to a self-convolution of the DOS (2e-DOS). In Fig. 9 (a) we plot this entity as a function of the two-particle binding energy. We recognize three prominent regions which we highlighted by the different shading. If two electrons from the 6p band are involved we label this region $p - p$, in an analogous fashion the other labels are to be understood. From simple energetic grounds one can observe only parts

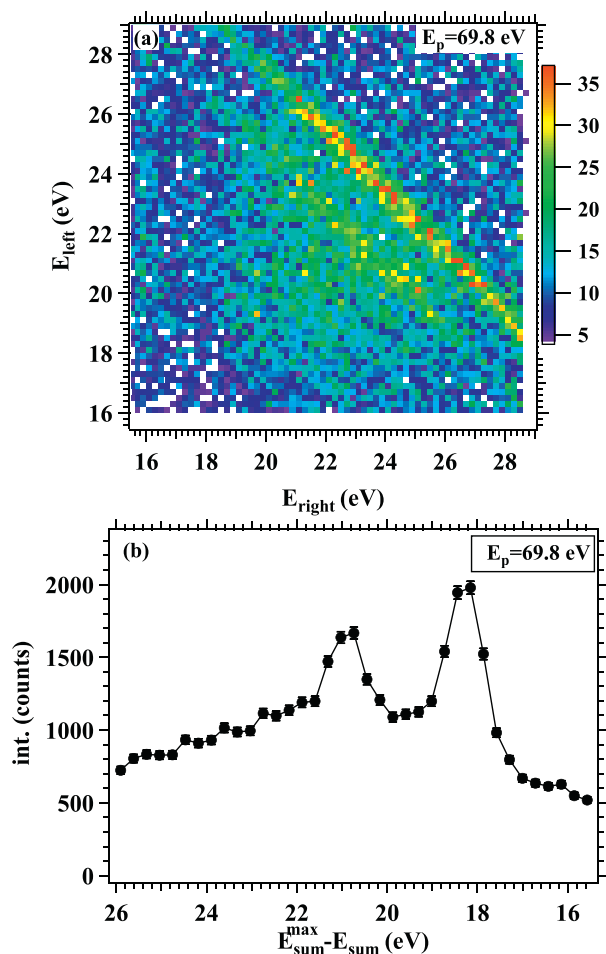


Fig. 6. In panel (a) we present the 2D-Energy distribution for an (e,2e) experiment with $E_p=69.8$ eV. Both spectrometers were set to capture events coming from a collision of the primary electron with the $5d$ core level. The sum energy spectrum is shown in (b).

of this line shape. We recall the binding energy of the $5d$ core levels with 20.58 and 17.93 eV, respectively. Furthermore, the work function has to be overcome for electron emission. This means the filling of the $5d_{3/2}$ ($5d_{5/2}$) vacancy will probe only up to a two-particle binding energy of 16.58 eV (13.93 eV). These energetic positions are marked by the pair of dashed arrows. In our experiments the lowest detectable kinetic energy was 6.5 eV. This further limits the range which is probed by the experiment as indicated by the pair of solid arrows.

In Fig. 9 we present the Auger line from the data shown in Fig. 8 (b). For these curves we selected the energy window to capture either the $5d_{3/2}$ or $5d_{5/2}$ photoelectron line within an energy window of ± 1 eV of the peak position of 23.5 and 26.1 eV, respectively. Near the cut-off energy the intensity of the $5d_{5/2}$ decay is higher than from the $5d_{3/2}$ decay which we associate with the filling of the $5d_{3/2}$ hole by a $5d_{5/2}$ electron. In such a scenario the emitted Auger electron has a lower kinetic energy by an amount given by the binding energy difference of the $5d$ core levels. In the case of Pb this amounts to 2.65 eV. The observed Auger line shapes differ significantly from the simple 2e-DOS. The 2e-DOS displays a double peak features at 5.2 and 3 eV, respectively. The experiment exhibits a broad maximum centered at 3.6 eV.

Introducing a finite value for the correlation strength U within the Cini-Sawatzky theory distorts the 2e-DOS such that spectral weight is moved to lower kinetic energies. This leads to even larger deviation from the experimental curve. Strictly speaking this theory is only valid for filled or almost filled valence bands. This does not hold for Pb, because there are still 4 vacancies in the $6p$ level. Additionally the spin-

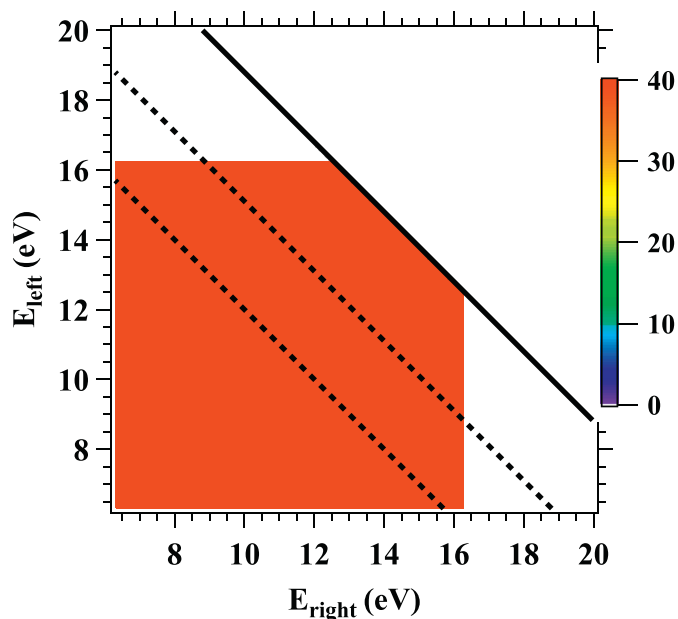


Fig. 7. The red area covers the part of the 2D-Energy window if the scattered primary is in a window from 6.3 to 14.8 eV, while the Auger electron has an energy from 6.3 to 16.3 eV. The primary energy is $E_p=32.8$ eV. The solid diagonal line indicates the position of E_{sum}^{max} . The pair of dashed lines show the position of the energy gap. The largest part of the gap region is covered and explains the observed intensity in Fig. 3 (a). (For interpretation of the references to colour in this figure legend, the reader is referred to the web version of this article.)

orbit interaction of the $6p$ levels can not be ignored. Clearly a more sophisticated treatment is required to explain the observed Auger line shape. Within the precision of the experiment both Auger curves show zero intensity at $E_{sum}^{max} - E_{sum} = 0$. This means the minimum energy required to emit two electrons equals twice the work function. This we take as a hint that the correlation energy is close to zero. Following the notation of Antonides et al. the effective electron-electron interaction is $U_{eff} \approx 0$ [18].

3.3. DPE from the valence band

In Fig. 10(a) we present the 2D-Energy spectrum for a photon energy of 48.4 eV. For the chosen spectrometer settings the $5d$ photoelectrons are almost out of the field of view. Near the E_{sum}^{max} line very few events are captured. Most of the intensity comes from the small portion of the $5d_{3/2}$ line within the spectrometer view and its inelastic tail. From Fig. 8 we recall that the high energy tail of the Auger electron extends up to 16 eV. The pair of red lines in both panels of Fig. 10 marks this energy cut-off and define a L-shaped region. Clearly, most of the intensity originates from the L-shaped region. For these events at least one electron does not exceed the Auger kinetic energy. The existence of an Auger electron is tied to the electron emission from a core level. This we have proven in previous section. Therefore the intensity within the L-shaped region is dominated by Auger-photoelectron coincidences in which the photoelectron has suffered energy losses. This statement is also true for the measurement with $h\nu=51$ eV, see Fig. 10(b). In this experiment the $5d$ photoelectron lines are now fully out of the field of view. In line with Fig. 10(a) the intensity is dominated by events within the L-shaped area.

The intensity due to DPE from the valence band without participation of the core levels must come outside the L-shaped region and is bounded by the E_{sum}^{max} line. In Fig. 10(a) this region amounts to 2.4% of the detected intensity while for Fig. 10(b) a value of 5.5% is found. The low intensity near the E_{sum}^{max} line can be better visualized by a E_{sum}

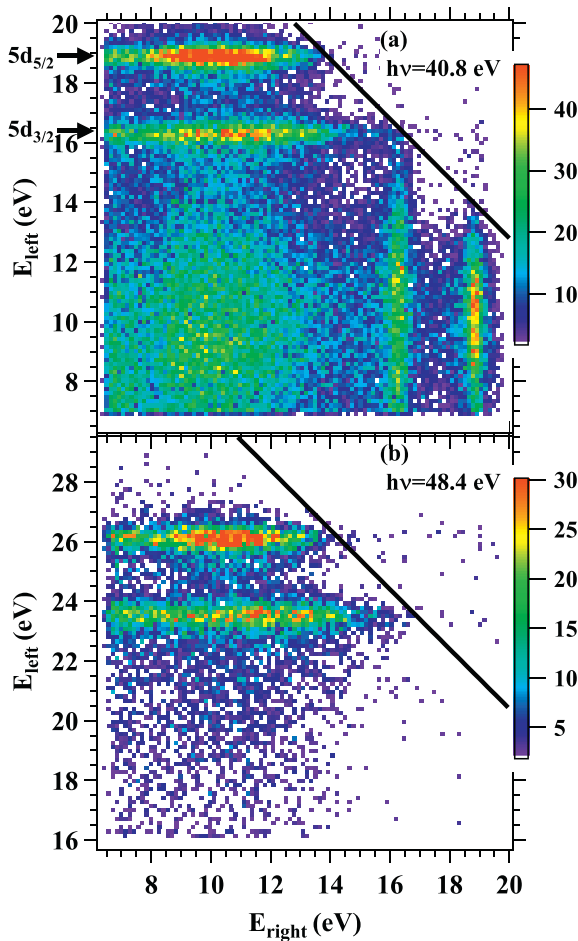


Fig. 8. 2D-Energy distribution for DPE obtained with $h\nu = 40.8$ eV in (a). The energy window of both spectrometer covers the energy of the Auger and $5d$ electron. In (b) the photon energy was 48.4 eV. In order to capture the Auger-photoelectron pairs with $h\nu = 48.4$ eV both spectrometer cover different energy intervals. The means the ‘left’ spectrometer detects the $5d$ electron while the ‘right’ spectrometer captures the Auger electron. The solid diagonal line indicates the position of E_{sum}^{max} .

spectrum. This is presented in Fig. 11 for the measurement with $h\nu = 51$ eV. We also used the constraint $E_{left} - E_{right} \leq 5$ eV. This selection we have visualized by a pair of dashed lines in Fig. 10(b). Only the intensity within the dashed lines is considered. The constraint on the energy difference was made in order reject intensity from the L-shaped region as much as possible while maintaining enough counts for a meaningful plot. In Fig. 11 we have added an arrow which indicates at which point intensity from the L-shaped region makes a contribution. If the $E_{sum}^{max} - E_{sum}$ is smaller than 5.2 eV the intensity has no contribution from the $5d$ core levels.

It is apparent that the intensity drops monotonically towards the high energy cut-off. The intensity vanishes, within the accuracy of the experiment, at $E_{sum}^{max} - E_{sum} = 0$. In other words there is no shift which indicates that the effective electron-electron interaction is close to zero. A low DPE intensity is consistent with the notion that the strength of the electron-electron interaction determines the intensity level. This in turn is reasonable, because the band structure of Pb is well-described by an effective single electron picture. In the absence of a theoretical DPE spectrum one may resort to the simplest picture. This leads to the 2e-DOS curve, added to Fig. 2, which completely ignores matrix element effects. The 2e-DOS curve displays two peaks at about 3 and 5 eV which are a consequence of the fine structure within the $6p$ band, see Fig. 2. At a binding energy of 7 eV the 2e-DOS displays a minimum close to zero. At this energy position the probability to eject two $6p$ electrons drops

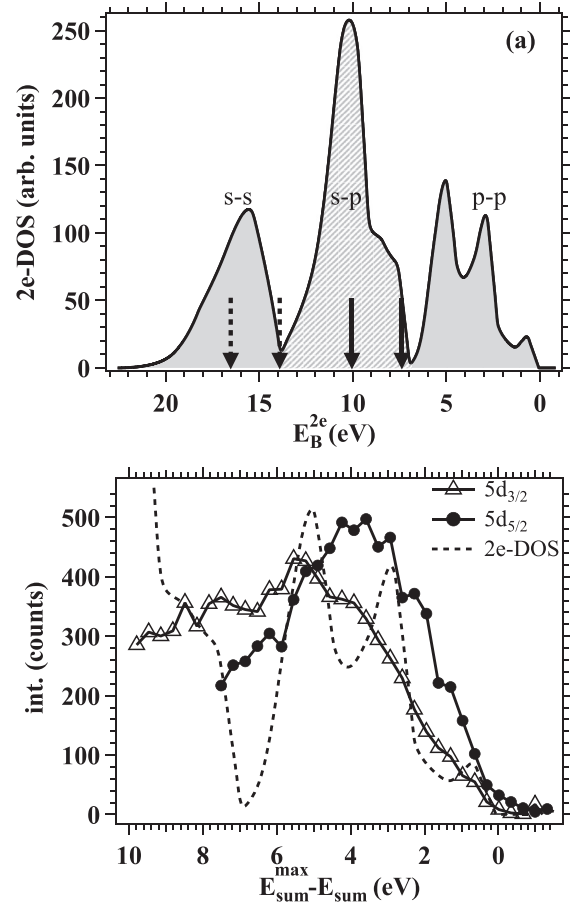


Fig. 9. In panel (a) we display the self-convolution of the DOS shown in Fig. 2. The pair of dashed arrows indicate the highest binding energy possible if the Auger electrons have zero kinetic energy. The pair of solid arrows mark the position if the Auger electrons have a minimum kinetic energy of 6.5 eV. Panel (b) shows the Auger line shape in coincidence with the $5d_{3/2}$ (triangles) and $5d_{5/2}$ (circles) photoelectrons. The photon energy is $h\nu = 48.4$ eV. The dashed curve is the self-convolution of the DOS shown in (a).

sharply, because one approaches the band gap, see Fig. 2. Compared to the experiment the 2e-DOS curve displays more structure.

3.4. Estimate of the Cooper pair emission rate

Superconductivity is a macroscopic quantum effect in which certain materials loose their resistivity upon cooling below a critical temperature. In the case of Pb this temperature is 7.2 K which is well below our measurement temperature of 300 K. For an explanation of the dissipation less current the concept of Cooper pairs was introduced. These pairs are formed by electrons which possess opposite momenta and spin. We want to assess whether the observation of Cooper pair emission via single photon absorption is feasible. It is immediately obvious that such an endeavor will be experimentally challenging, because only a small fraction of the electrons form Cooper pairs.

A theoretical framework of this process has been developed already which presents numerical examples for s-wave pairing [8,9]. In this case the emitted Cooper pairs have a characteristic energy signature in which their energy sum is close to E_{sum}^{max} within a range given by the superconducting energy gap. This is of the order of a few meV. Additionally the two electrons are supposed to have equal energies within a width given by the energy gap. This means we expect intensity due to Cooper pairs at the position marked by the red circle of Fig. 10 (b). Furthermore, the emission directions of the two electrons lie within a

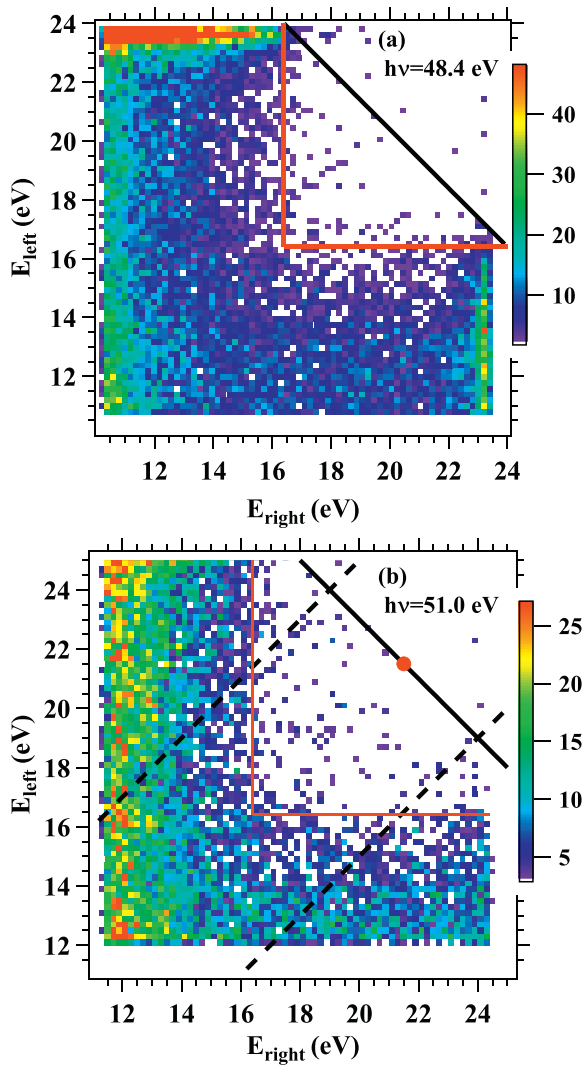


Fig. 10. 2D-Energy distribution for DPE obtained with $h\nu = 48.4$ eV in (a) and 51.0 eV in (b). The solid diagonal line indicates the position of E_{sum}^{max} . The red circle marks the position where Cooper pair emission is theoretically predicted [8]. The pair of dashed diagonal lines in (b) marks the energy region used for the calculation of the E_{sum} spectrum shown in Fig. 11. (For interpretation of the references to colour in this figure legend, the reader is referred to the web version of this article.)

plane perpendicular to the surface. The emission angles with respect to the normal are identical, but the emitted electrons propagate in opposite directions. This is an immediate consequence of the energy and in-plane momentum conservation of the DPE process and the fact that the two electrons constituting a Cooper pair have opposite momenta [8]. The maximum intensity is predicted for emission angles of $\pm 45^\circ$ with respect to the normal with an angular spread of about $\pm 5^\circ$. From this point of view our experimental geometry is perfectly suited for Cooper pair emission. Theory predicts an intensity contribution from Cooper pairs which exceeds those of normal pairs by 2–3 orders of magnitude in the small region of parameter space. The rate of normal pairs we have determined at 300 K. For the normal pairs only a weak temperature dependence is expected.

This allows us to estimate the count rates for Cooper pair emission in the following way. First we assume an energy gap of 5 meV which is the value for V_3Si . This material was discussed in the theory [8,9]. Next we determine the count rate of regular DPE within 2 eV of E_{sum}^{max} , while the energy difference was within ± 3 eV. This result was scaled to a window of size $5 \text{ meV} \times 5 \text{ meV}$ near E_{sum}^{max} . Using the data displayed in

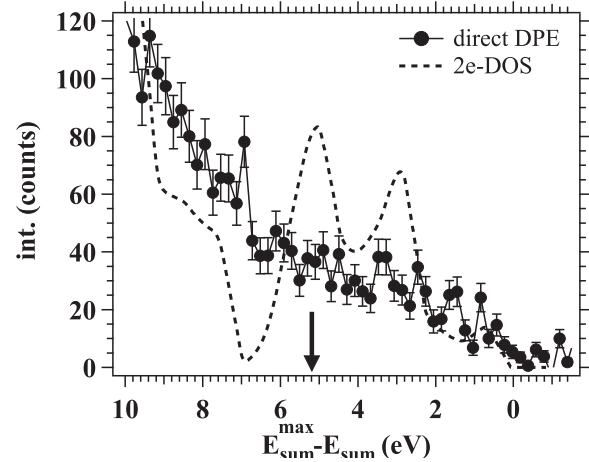


Fig. 11. We show as solid curve the E_{sum} spectrum obtained from the data presented at Fig. 10(b). For comparison we have added the self-convolution of the DOS as dashed curve. The arrow indicates the energy position below which Auger photoelectron pairs make a contribution.

Fig. 10(a) we find a value of 1.5×10^{-10} cps. This value was obtained at 300 K and we scale it with the theoretically predicted increase in the emission probability of about 10^3 in the superconducting state. Hence we arrive at a Cooper pair emission rate of 1.5×10^{-7} cps. This means the detection of 1000 Cooper pairs takes about 125 years to complete. This is clearly a formidable obstacle for a successful experiment. As mentioned above coincidence spectroscopy requires a low primary flux in order to keep the random coincidences at an acceptable level. Therefore increasing the primary flux is not an option. A tremendous increase in the detection efficiency is possible if the solid angle is increased, because the pair emission scales quadratically with the solid angle [4,46]. Our spectrometer captures electrons within 1% of the half space. Recent developments by using the high acceleration voltage of a PEEM lens have achieved the detection of the full half space [47–50]. This leads to an increase of the coincidence rate of about 10^4 . Such a PEEM lens has been coupled to two hemispherical analyzers in series. In this case the transit time differences until the detector is hit are expected to be about 1 ns [51]. This expectation is experimentally met as DPE experiments with such an instrument demonstrate [47]. This is significantly better than the value for our spectrometer which amounts to about 10 ns [12,13]. Therefore one can increase the primary flux by a factor of 10 while maintaining the same ratio of true to random coincidences. A very recent evolution of the concept of a PEEM lens was developed for high resolution spin-resolved photoemission with an ultimate resolution of 12 meV [48]. If we keep these established improvements in mind we arrive at 0.45 days to detect 1000 Cooper pairs. This amounts to a rate of 0.03 cps and this puts Cooper pair detection within reach. A number of 1000 Cooper pairs may suffice to prove the existence of the effect, though much more events are needed to do spectroscopy to unravel aspects of superconductivity. It appears questionable that DPE will become a tool to study superconductivity.

4. Summary

We provided a comprehensive study on the pair emission from a Pb surface. From the (e,2e) experiments we have learned that the density-of-states gives a reasonable description of the intensity distribution. Nevertheless, intensity which energetically appears in the gap between the 6s and 6p region clearly demonstrates that shallow core levels need to be considered. These lead to auto-ionizing/Auger transitions not covered by theory. We prove the existence of the low energy Auger electrons via complementary DPE experiments. In these studies the intensity is mainly given by Auger-photoelectron pairs, which are about

an order of magnitude larger than the emission directly from the valence band. From the Auger lineshape we determine that the effective Coulomb correlation U_{eff} is close to zero. The DPE intensity without participation of core levels is about an order of magnitude smaller than the Auger-photoelectron pairs.

Using our experimental data and theoretical predictions we make an estimate of the Cooper pair emission rate. It is found that the instrumentation used in this work is not capable to detect this effect. The availability of a new class of electron spectrometer provides an improvement of several orders of magnitude. In this way the detection of the effect may be possible. The development of DPE as tool to study superconductivity remains questionable.

Acknowledgment

Funding from the German Research Foundation within the Collaborative Research Centre 762 (project B7) is gratefully acknowledged.

References

- [1] H.W. Haak, G.A. Sawatzky, T.D. Thomas, Auger-photoelectron coincidence measurements in copper, *Phys. Rev. Lett.* 41 (26) (1978) 1825.
- [2] C.A. Creagh, S.M. Thurgate, The use of auger photoelectron coincidence spectroscopy to deconvolute the $m_{45}n_{45}n_{45}$ AES of palladium, *J. Electron. Spectrosc. Relat. Phenom.* 69 (2001). 114?116.
- [3] G.A. van Riessen, S.M. Thurgate, Auger photoelectron coincidence spectroscopy: simplifying complexity, *Surf. Interface Anal.* 38 (4) (2006) 691–698.
- [4] E. Jensen, R.A. Bartynski, S.L. Hulbert, E. Johnson, Auger photoelectron coincidence spectroscopy using synchrotron radiation, *Rev. Sci. Instrum.* 63 (1992) 3013.
- [5] R. Gotter, A. Ruocco, A. Morgante, D. Cvetko, L. Floreano, F. Tommasini, G. Stefani, The ALOISA end station at eletra: a novel multicoincidence spectrometer for angle resolved APECS, *Nucl. Instrum. Methods A* 1468 (Part 2) (2001) 467–468.
- [6] F.O. Schumann, Y. Aliaev, I. Kostanovskiy, G.D. Filippo, Z. Wei, J. Kirschner, Electron pair emission from surfaces: intensity relations, *Phys. Rev. B* 93 (23) (2016) 235128.
- [7] B.D. Nappitu, J. Berakdar, Two-particle photoemission from strongly correlated systems: a dynamical mean-field approach, *Phys. Rev. B* 81 (19) (2010) 195108.
- [8] K.A. Kouzakov, J. Berakdar, Photoinduced emission of cooper pairs from superconductors, *Phys. Rev. Lett.* 91 (2003) 257007.
- [9] K.A. Kouzakov, J. Berakdar, Mechanisms of superconductivity studied by two-pmission, *J. Electron. Spectrosc. Relat. Phenom.* 161 (1–3) (2007) 121.
- [10] K.A. Kouzakov, J. Berakdar, Spectroscopy of electron correlations in superconductors, *Philos. Mag.* 86 (17–18) (2006) 2623–2630.
- [11] G.A. van Riessen, F.O. Schumann, M. Birke, C. Winkler, J. Kirschner, Correlated positron-electron emission from surfaces, *J. Phys.* 20 (44) (2008) 442001.
- [12] G.A. van Riessen, Z. Wei, R.S. Dhaka, C. Winkler, F.O. Schumann, J. Kirschner, Direct and core-resonant double photoemission from cu(001), *J. Phys.: Condens. Matter* 22 (9) (2010) 092201.
- [13] F.O. Schumann, R.S. Dhaka, G.A. van Riessen, Z. Wei, J. Kirschner, Surface state and resonance effects in electron pair emission from cu(111), *Phys. Rev. B* 84 (2011) 125106.
- [14] Light source mbs 1-1 from mb scientific.
- [15] Monochromator VUV5040 from VG scienta.
- [16] G.A. Sawatzky, Auger photoelectron coincidence spectroscopy, in: C.L. R. P. M. Bryant (Ed.), *Auger Electron Spectroscopy*, Academic Press, San Diego, 1988.
- [17] D. Iablonskiy, M. Patanen, S. Aksela, H. Aksela, Changes in the 5d photoionization spectra between atomic and solid pb, *Phys. Rev. B* 86 (4) (2012) 041101.
- [18] E. Antonides, E.C. Janse, G.A. Sawatzky, LMM Auger spectra of cu, zn, ga, and ge. i. transition probabilities, term splittings, and effective coulomb interaction, *Phys. Rev. B* 15 (4) (1977) 1669.
- [19] J.L. Powell, B. Crasemann, *Quantum Mechanics*, Dover, 2015.
- [20] J. Berakdar, Emission of correlated electron pairs following single-photon absorption by solids and surfaces, *Phys. Rev. B* 58 (1998) 9808.
- [21] K. Würde, A. Mazur, J. Pollmann, Surface electronic structure of pb(001), pb(110), and pb(111), *Phys. Rev. B* 49 (11) (1994) 7679.
- [22] J. Berakdar, H. Gollisch, R. Feder, Pair correlation in two-electron emission from surfaces, *Solid State Commun.* 112 (10) (1999) 587.
- [23] R. Feder, H. Gollisch, D. Meinert, T. Scheunemann, O.M. Artamonov, S.N. Samarin, J. Kirschner, Low-energy (e,2e) spectroscopy from the w(001) surface: experiment and theory, *Phys. Rev. B* 58 (1998) 16418.
- [24] H. Gollisch, X. Yi, T. Scheunemann, R. Feder, Spin-polarized low-energy (e, 2e) spectroscopy of non-magnetic surfaces, *J. Phys.: Condens. Matter* 11 (48) (1999) 9555.
- [25] U. Rücker, H. Gollisch, R. Feder, Electron-induced two-electron emission from ultrathin magnetic films, *Phys. Rev. B* 72 (2005) 214424.
- [26] H. Gollisch, N.v. Schwartzberg, R. Feder, Emission of correlated electron pairs from solid surfaces, *Phys. Rev. B* 74 (2006) 075407.
- [27] F.O. Schumann, L. Behnke, C.H. Li, J. Kirschner, Y. Pavlyukh, J. Berakdar, Electron pair emission from a highly correlated material, *Phys. Rev. B* 86 (3) (2012) 035131.
- [28] Z. Wei, F.O. Schumann, R.S. Dhaka, J. Kirschner, Electron pair emission from surfaces: diffraction effects, *Phys. Rev. B* 85 (19) (2012) 195120.
- [29] L. Ley, R. Pollak, S. Kowalczyk, D.A. Shirley, The onset of relativistic effects in the density of states of the 6s6p elements tl, pb, and bi, *Phys. Lett. A* 41 (5) (1972) 429.
- [30] K. Horn, B. Reihl, A. Zartner, D.E. Eastman, K. Hermann, J. Noffke, Electronic energy bands of lead: angle-resolved photoemission and band-structure calculations, *Phys. Rev. B* 30 (4) (1984) 1711.
- [31] G. Jezequel, A. Barski, P. Steiner, F. Solal, P. Roubin, R. Pinchaux, Y. Petroff, Indirect transitions in angle-resolved photoemission, *Phys. Rev. B* 30 (8) (1984) 4833.
- [32] G. Jézéquel, I. Pollini, Experimental band structure of lead, *Phys. Rev. B* 41 (3) (1990) 1327.
- [33] S.N. Samarin, J. Berakdar, O.M. Artamonov, J. Kirschner, Visualizing spin-dependent electronic collisions in ferromagnets, *Phys. Rev. Lett.* 85 (2000) 1746.
- [34] S. Samarin, O.M. Artamonov, A.D. Sergeant, J. Kirschner, A. Morozov, J.F. Williams, Spin-orbit coupling in tungsten by spin-polarized two-electron spectroscopy, *Phys. Rev. B* 70 (2004) 073403.
- [35] R. Feder, H. Gollisch, Selection rules in (e,2e) spectroscopy from surfaces, *Solid State Commun.* 119 (10–11) (2001) 625.
- [36] H. Gollisch, R. Feder, Selection rules in (e, 2e) spectroscopy from ferromagnetic surfaces, *J. Phys.* 16 (2004) 2207.
- [37] G.D. Filippo, F.O. Schumann, S. Patil, Z. Wei, G. Stefani, G. Fratesi, M.I. Trioni, J. Kirschner, Electron coincidence studies of sulfur-overlayers on cu(001) and ni(001) surfaces, *J. Electron. Spectrosc. Relat. Phenom.* 211 (2016) 32.
- [38] S.P. Kowalczyk, R.A. Pollak, F.R. McFeely, L. Ley, D.A. Shirley, $L_{2,3}m_{45}n_{45}$ auger spectra of metallic copper and zinc: theory and experiment, *Phys. Rev. B* 8 (6) (1973) 2387.
- [39] G.A. Sawatzky, Quasiatomic auger spectra in narrow-band metals, *Phys. Rev. Lett.* 39 (8) (1977) 504.
- [40] A.C. Parry-Jones, P. Weightman, P.T. Andrews, The $m_{4,5}n_{4,5}n_{4,5}$ auger spectra of ag, cd, in and sn, *J. Phys. C* 12 (8) (1979) 1587.
- [41] R.J. Cole, C. Verdozzi, M. Cini, P. Weightman, Off-site interactions in the CVV auger spectrum of noble metals: a study of silver, *Phys. Rev. B* 49 (19) (1994) 13329.
- [42] E. Jung, H.Q. Zhou, J.H. Kim, S. Starnes, R. Venkataraman, A.H. Weiss, Background-free auger line shape of ag $n_{2,3}VV$ measured with positron annihilation induced auger electron spectroscopy, *Appl. Surf. Sci.* 116 (1997) 318.
- [43] E. Jensen, R.A. Bartynski, S.L. Hulbert, E.D. Johnson, R. Garrett, Line narrowing in photoemission by coincidence spectroscopy, *Phys. Rev. Lett.* 62 (1) (1989) 71.
- [44] R. Gotter, A. Ruocco, M.T. Butterfield, S. Iacobucci, G. Stefani, R.A. Bartynski, Angle-resolved auger-photoelectron coincidence spectroscopy (AR-APECS) of the ge(100) surface, *Phys. Rev. B* 67 (3) (2003) 033303.
- [45] M. Cini, Two hole resonances in the XVV auger spectra of solids, *Solid State Commun.* 24 (9) (1977) 681.
- [46] H.W. Haak, G.A. Sawatzky, L. Ungier, J.K. Gimzewski, T.D. Thomas, Core-level electron-electron coincidence spectroscopy, *Rev. Sci. Instrum.* 55 (1984) 696.
- [47] B. Krömker, M. Escher, D. Funnemann, D. Hartung, H. Engelhard, J. Kirschner, Development of a momentum microscope for time resolved band structure imaging, *Rev. Sci. Instrum.* 79 (5) (2008) 7–053702.
- [48] C. Tusche, A. Krasnyuk, J. Kirschner, Spin resolved band structure imaging with a high resolution momentum microscope, *Ultramicroscopy* 159 (2015) 520.
- [49] D. Kutnyakhov, S. Chernov, K. Medjanik, R. Wallauer, C. Tusche, M. Ellguth, S.A. Nepijko, M. Krivenkov, J. Braun, S. Borek, J. Minár, H. Ebert, H.J. Elmers, G. Schönhense, Spin texture of time-reversal symmetry invariant surface states on (110), *Sci. Rep.* 6 (2016) 29394.
- [50] G. Schönhense, K. Medjanik, H.J. Elmers, Space-, time- and spin-resolved photoemission, *J. Electron. Spectrosc. Relat. Phenom.* 200 (2015) 94.
- [51] M. Escher, N. Weber, M. Merkel, C. Ziethen, P. Bernhard, G. Schönhense, S. Schmidt, F. Forster, F. Reinert, B. Krömker, D. Funnemann, 9NANOESCA: A novel energy filter for imaging x-ray photoemission spectroscopy, *J. Phys.* 17 (2005) S1329.